Measurement of Electric Parameters for thin materials

Toshihide Tosaka[1] Isamu Nagano[1] Satoshi Yagitani[1] Yoshiyuki Yoshimura[2]

[1]Graduate School of Natural Science and Technology, Kanazawa University

[2] Industrial Research Institute of Ishikawa

E-mail: tosaka@reg.ec.t.kanazawa-u.ac.jp

Abstract: One of the effective measures for shielding an electromagnetic wave is using shielding materials. For the design of shielding materials, it is important to know about the propagation of electromagnetic waves. For numerical analysis, it is necessary to know about the electric parameters. If we know about the material, we can use nominal values. But many of the electric parameters of materials are not known. We developed a shield box for measuring the shielding efficiency (*SE*). Here we propose a method to estimate unknown electric parameters of shielding materials by using the *SE* measurement system and numerical calculations. This is the first time the presumption of electric parameters is applied to the efficient design of an electromagnetic shield seat.

Key words: Sommerfeld, electric parameters, shield, presumption

1. Introduction

Recently, the use of electromagnetic waves is increasing in the technology of electronics, information, and communication. It is believed that electromagnetic wave leaks from electronic devices may cause incorrect operation of other electronic devices and may be a bad influence on the human body. Therefore it is necessary to consider an electromagnetic shield seat that can intercept an electromagnetic wave that leaks from some electronic devices.

An electromagnetic shield seat is a thin cloth that is covered by metal plating. Since the surface is uneven and no presumption system exists for this case, we could not determine the electrical parameters ($\varepsilon_r, \mu_r, \sigma$). But it is important to know about these parameters, because they decide the rate of interception of an electromagnetic wave.

In this study, we developed a presumption system for the electric parameters of thin cloth that was not previousing available. We presumed the electric parameters of the thin material and evaluated this system using known parameters.

2.Electromagnetic field analysis using a dipole source inside a multi-layered medium

If the distance z from the observation point to a source with wave length λ is $z \gg \lambda/2\pi$, the radiated field is the dominant wave emitted from the source and can be regarded as a plane wave. In this case, the shielding efficiency (*SE*) of the shielding material is not related to the position of the source. But the distance of the source from the observation point is $z \ll \lambda/2\pi$, and it can not be considered that the radiated field is the wave emitted from source. Thus it is necessary to calculate the electromagnetic field of a near source when calculating *SE*.

In this study in consideration of the source, we used the Sommefeld integral that expresses spherical waves by composition of cylindrical waves.

2.1 Analytical model and coordinate system

The coordinate system of a multi-layered model assuming an infinite plate is shown in Fig.1. A magnetic dipole source is assumed at z=h, with homogeneous layers above and below the dipole. In the diagram, Π_m denotes the Hertz vector. Superscripts identify the up-going wave (u), the down-going wave (d), and the direct wave (p), while subscripts indicate the layers.

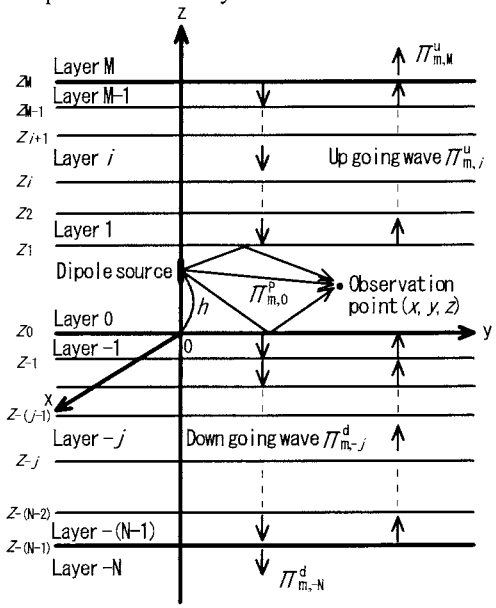

Fig.1. Multi-layered material model

2.2 Boundary conditions

The electromagnetic field can be found from Eqs.

(1) and (2) by using the Hertz vectors related to the magnetic dipole. In addition, ignoring time dependence, Π_m can be expressed as in Eq. (3).

$$\boldsymbol{E} = -\mathrm{j}\omega\mu\nabla \times \Pi_m \tag{1}$$

$$\boldsymbol{H} = \nabla\nabla \cdot \Pi_m + \mathrm{k}^2 \Pi_m \tag{2}$$

$$\Pi_m = \frac{\mathrm{nSI}}{4\pi}\frac{\mathrm{e}^{-\mathrm{jkR}}}{\mathrm{R}}\mathbf{i}_z \tag{3}$$

Here $\boldsymbol{E}$ is the electric field, $\boldsymbol{H}$ is the magnetic field, ω is the angular frequency, μ is the magnetic permeability, k is $\omega\sqrt{\varepsilon\mu}$, ε is the complex electric constant, n is the number of turns, S is the loop area, I is current, and R is the distance from the wave source. In Eq. (3), **j** is complex and $\mathbf{i}_z$ is the element of the vector that is in the z direction.

The boundary conditions between layers i and i+1 on the XY-plane may be expressed as in Eqs. (4) and (5) by applying the continuity of the electric field's tangential component to Eqs. (1) and (2).

$$\mu_i \Pi_{m,i} = \mu_{i+1}\Pi_{m,i+1} \tag{4}$$

$$\frac{\partial \Pi_{m,i}}{\partial z} = \frac{\partial \Pi_{m,i+1}}{\partial z} \tag{5}$$

These are expressed by Hertz vectors $\Pi_{m,I}$ for layer i and $\Pi_{m,i+1}$ for layer i+1.

2.3 Application of boundary conditions

2.3.1 Layers above the source

Using the Sommerfeld representation to express a spherical wave by synthesis of cylindrical waves, Eq. (3) can be transformed into Eq. (6) for the up-going wave and into Eq. (7) for the down-going wave in layer i. In addition, the sum of two waves gives the Hertz vector for layer i as in Eq. (8).

$$\Pi^u_{m,i} = \frac{\mathrm{nSI}}{4\pi}\int_0^\infty F^u_{m,i}(\lambda)J_0(\lambda r)\mathrm{e}^{-\nu_i(z-z_i)}\lambda \mathrm{d}\lambda \tag{6}$$

$$\Pi^d_{m,i} = \frac{\mathrm{nSI}}{4\pi}\int_0^\infty F^d_{m,i}(\lambda)J_0(\lambda r)\mathrm{e}^{\nu_i(z-z_i)}\lambda \mathrm{d}\lambda \tag{7}$$

$$\text{Here, } \nu_i = \sqrt{\lambda^2 - \mathrm{k}_i^2}$$

$$\Pi_{m,i} = \Pi^u_{m,i} + \Pi^d_{m,i} \tag{8}$$

F_m is an unknown function of the constant of integration λ, with the subscripts and superscripts the same as for Π_m. In addition, J_0 is a zero-order Bessel function of the first kind, r is the radial distance in cylindrical coordinates, and z_i is the distance to layer i along the z-axis.

By taking $z=z_{i+1}$, and substituting $\Pi_{m,I}$ and $\Pi_{m,i+1}$ of Eq.(8) into Eqs. (4) and (5), the unknown $F_m(\lambda)$ can be expressed by a matrix as shown in Eq. (9).

$$\begin{bmatrix} F^u_{m,i} \\ F^d_{m,i} \end{bmatrix} = \frac{1}{2\mu_i\nu_i}\begin{bmatrix} (\mu_{i+1}\nu_i + \mu_i\nu_{i+1})\mathrm{e}^{\nu_i h_i} & (\mu_{i+1}\nu_i - \mu_i\nu_{i+1})\mathrm{e}^{-\nu_i h_i} \\ (\mu_{i+1}\nu_i - \mu_i\nu_{i+1})\mathrm{e}^{\nu_i h_i} & (\mu_{i+1}\nu_i + \mu_i\nu_{i+1})\mathrm{e}^{-\nu_i h_i} \end{bmatrix}\begin{bmatrix} F^u_{m,i+1} \\ F^d_{m,i+1} \end{bmatrix}$$

$$\text{Here, } h_i = z_{i+1} - z_i$$

$$= \begin{bmatrix} c_{i11} & c_{i12} \\ c_{i21} & c_{i22} \end{bmatrix}\begin{bmatrix} F^u_{m,i+1} \\ F^d_{m,i+1} \end{bmatrix} \tag{9}$$

First, the unknown λ is eliminated.

Eq. (9) is a recurrence expression with the known 2 × 2 matrix including c_{11}, c_{12}, c_{21}, c_{22} being a coefficient; expanding from layer 0 to layer M gives Eq. (10).

$$\begin{bmatrix} F^u_{m,0} \\ F^d_{m,0} \end{bmatrix} = \prod_{i=0}^{M-1}\begin{bmatrix} c_{i11} & c_{i12} \\ c_{i21} & c_{i22} \end{bmatrix}\begin{bmatrix} F^u_{m,M} \\ 0 \end{bmatrix} - \frac{1}{\nu_0}\begin{bmatrix} \mathrm{e}^{\nu_0 h} \\ 0 \end{bmatrix}$$

$$= \begin{bmatrix} C_{11} & C_{12} \\ C_{21} & C_{22} \end{bmatrix}\begin{bmatrix} F^u_{m,M} \\ 0 \end{bmatrix} + \begin{bmatrix} C \\ 0 \end{bmatrix} \tag{10}$$

Here C_{11}, C_{12}, C_{21}, C_{22} are components of the known matrices.

2.3.2 Layers below the source

In this case, too, the continuity of the electric field's tangential component involves Eq. (11) at the boundary $z=z_{-j}$, and recursive Eq. (12) can be derived.

$$\begin{bmatrix} F^u_{m,-j} \\ F^d_{m,-j} \end{bmatrix} = \frac{1}{2\mu_{-j}\nu_{-j}}\begin{bmatrix} (\mu_{-(j+1)}\nu_{-j} + \mu_{-j}\nu_{-(j+1)})\mathrm{e}^{\nu_{-j}h_{-j}} & (\mu_{-(j+1)}\nu_{-j} - \mu_{-j}\nu_{-(j+1)})\mathrm{e}^{-\nu_{-j}h_{-j}} \\ (\mu_{-(j+1)}\nu_{-j} - \mu_{-j}\nu_{-(j+1)})\mathrm{e}^{\nu_{-j}h_{-j}} & (\mu_{-(j+1)}\nu_{-j} + \mu_{-j}\nu_{-(j+1)})\mathrm{e}^{-\nu_{-j}h_{-j}} \end{bmatrix}\begin{bmatrix} F^u_{m,-(j+1)} \\ F^d_{m,-(j+1)} \end{bmatrix}$$

$$\text{Here, } h_{-j} = z_{-j} - z_{-(j-1)}$$

$$= \begin{bmatrix} c'_{-j11} & c'_{-j12} \\ c'_{-j21} & c'_{-j22} \end{bmatrix}\begin{bmatrix} F^u_{m,-(j+1)} \\ F^d_{m,-(j+1)} \end{bmatrix} \tag{11}$$

$$\begin{bmatrix} F^u_{m,0} \\ F^d_{m,0} \end{bmatrix} = \prod_{j=0}^{-(N-1)}\begin{bmatrix} c'_{j11} & c'_{j12} \\ c'_{j21} & c'_{j22} \end{bmatrix}\begin{bmatrix} 0 \\ F^d_{m,-N} \end{bmatrix} - \frac{1}{\nu_0}\begin{bmatrix} 0 \\ \mathrm{e}^{-\nu_0 h} \end{bmatrix}$$

$$= \begin{bmatrix} C'_{11} & C'_{12} \\ C'_{21} & C'_{22} \end{bmatrix}\begin{bmatrix} 0 \\ F^d_{m,-N} \end{bmatrix} + \begin{bmatrix} 0 \\ C' \end{bmatrix} \tag{12}$$

2.4 Calculation of unknowns

The unknowns found above for the zero layer must be equivalent; that is, Eq. (10) equals Eq. (12). Therefore, the unknowns for the top layer M and

$$F^u_{m,M} = \frac{C'_{12}C' + C'_{22}C}{C_{21}C'_{12} - C_{11}C'_{22}} \tag{13}$$

$$F^d_{m,-N} = \frac{C_{11}C' + C_{21}C}{C_{21}C'_{12} - C_{11}C'_{22}} \tag{14}$$

bottom layer -N are as follows.

The unknowns for all other layers can be found by substituting the obtained values into the recurrence expression and performing repeated calculations. Thus, Π_m can be determined for every layer. Then the electromagnetic field in every layer can be determined by substituting Π_m into Eqs. (1) and (2).

2.5 Numerical calculation algorithm

There are various methods for numerical calculation of the semi-infinite Sommerfeld integral. In this calculation, however, the trapezoidal rule is

employed for simplicity. Since the integral converges as the numerical calculation proceeds, the processing in terminated as soon as the increment falls bellow 10^{-9}. In addition, the electromagnetic field in Eqs. (1) and (2) is found by numerical differentiation of Π_m by the central finite difference method.

In the analysis used in this study, the electromagnetic field can be calculated both in the vicinity of a magnetic dipole wave source and far away from it because the Hertz vectors are taken into account.

3. Measurement using a shield box

In this study, we used a measurement system of shield efficiency as shown in Fig.2. A shield box was made from 3mm thick copper (Cu) plate.

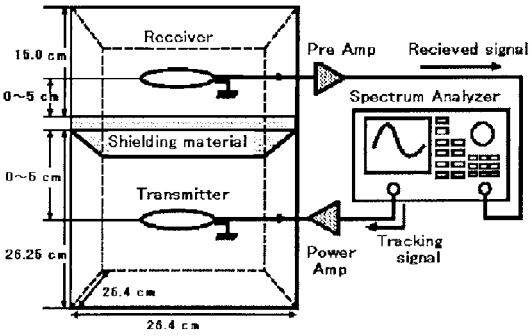

Fig.2. Measurement system of shielding efficiency

Shielding material was placed in the middle part of the box and the *SE* was estimated as the ratio of the magnetic field strength at the observation point without the shielding material (H_0) to that with the shielding material (Hs):

$$SE = 20\log_{10}\frac{|H_0|}{|H_S|} \text{ [dB]} \qquad (15)$$

If the transmitted magnetic field from the source was observed through a side plane, an upper plane, or a lower plane of the shield box, we could not accurately find the shielding efficiency of that material. Therefore, the influence of the circumference of the shield box is taken into consideration.

To do this, we carried out a computer simulation to calculate the attenuation of the transmitted magnetic field outside the shield box. The set up and results are shown in Fig.3.1 and Fig.3.2. All transmitted signals outside the box were attenuated 30dB or more. Thus any transmitted signal that returns through the side or upper or lower plane would be attenuated even more. Thus, theoretically, we can ignore the influence of the circumference of the shield box.

However, the scale of the shield box is limited and we must consider that effect. Fig.4 shows experimentally the effect the type and the difference of the area of the shielding material has on *SE*. And it appears that there is no effect from the side of the shield box because the *SE* of a 20cm×20cm piece of each type of shielding material is not different from a 15cm×15cm piece of that same type.

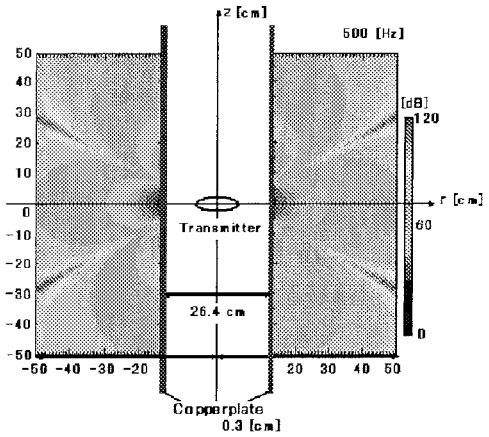

Fig.3.1. Attenuation of the transmitted magnetic field by the side of shield box

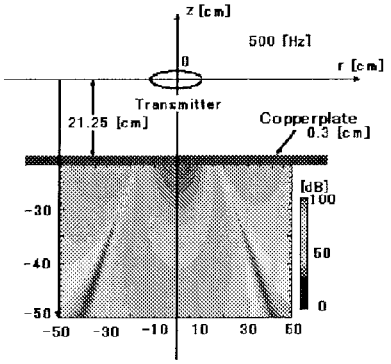

Fig.3.2. Attenuation of the transmitted magnetic field by the lower plane of shield box

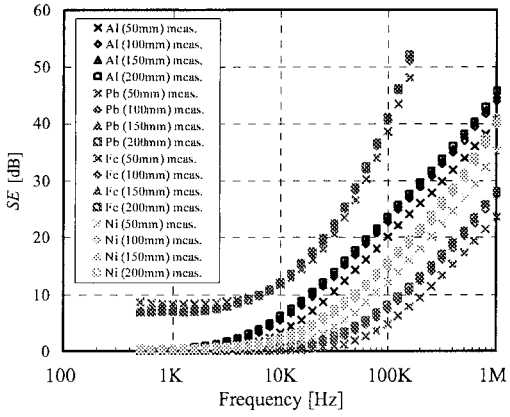

Fig.4. Difference of the type and area of shielding

4. Presumption method of electric parameters

The *SE* calculations are most influenced by the electric parameters. *SE* has different characteristics with electric parameters of different types of materials and characteristic curves can be drawn for each type (Fig.4). For example, we see that only the *SE* of ferromagnetic shielding can be observed at low

frequency.

When the presumption of electric parameters technique is used, electric parameters are calculated by bringing *SE* close to the experimental values. The electric parameters are changed in order, and the difference between the analytic values and the experimental values is made as small as possible. The *SE* is at its presumption value when it is closest to the experimental values. In this study, the least square method was used as the method to get close to the experimental values.

Until now, this system was not available to estimate the electric parameters for ferromagnetic material, because the calculated *SE* was not in agreement with the measured value in the frequency range of interest. We considered the possibility that the transmitter current changed as one of the causes. How the transmitter current changed for different materials was investigated and is shown in Fig.5. Regardless of the material, it did not change. We then found out that by taking into account the frequency characteristic of the permeability of the materials, the presumption of electric parameters, for not only diamagnetic material but also for ferromagnetic material, could be attained.

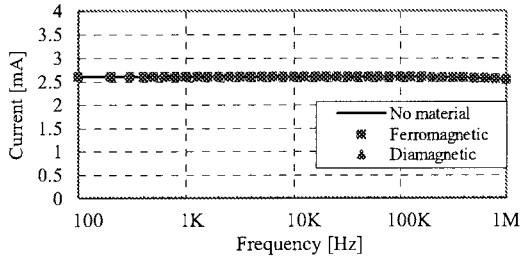

Fig.5. Transmitter current

5. Presumed result

In this study, we tested the presumption of electric parameters technique by using materials that had known electric parameters beforehand. We were able to evaluate the accuracy of the presumed result by comparing the *SE* of the analytic value and the experimental value as is shown in Fig.6. We used the nominal electric parameter values for the numerical analysis. From this figure, we see that the experimental values and the analytic values are nearly the same.

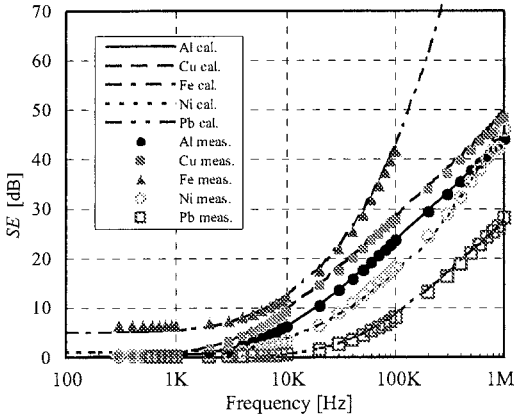

Fig.6. Shielding effect of magnetic field

Then, we can presume the electric parameters from this approximation. Table 1 compares the nominal values and the electric parameters that are presumed from this method.

Table 1. Nominal electric parameter values compared to presumed values

material [thickness]	εr [nom./cal.]	μr [nom./cal.]	σ [nom./cal.]
Al (0.1mm)	1.0/1.0	1.0/1.0	3.63 X 10^7 / 3.51 X 10^7
Cu (0.11mm)	1.0/1.0	1.0/1.0	5.80 X 10^7 / 5.19 X 10^7
Pb (0.11mm)	1.0/1.0	1.0/1.0	5.00 X 10^6 / 5.00 X 10^6
Fe (0.25mm)	1.0/1.0	140.0/80.0～115.0	1.02 X 10^7 / 0.92 X 10^7
Ni (0.1mm)	1.0/1.0	50.0/5.0～12.0	1.45 X 10^7 / 2.00 X 10^7

6. Conclusion

This research studied a method to estimate unknown electric parameters of shielding materials by using the *SE* measurement system and numerical calculations. We did an electromagnetic field analysis of a magnetic dipole placed inside a multi-layered medium. Our numerical analysis used the Sommerfeld representation of spherical waves by integration of cylindrical waves. We investigated the effects of the return of the transmitter signals through a side plane, an upper plane, and a lower plane of the shield box. We found no influence on the measuring of *SE* from external sources because no waves left the shield box and no waves returned to the shield box.

We determined presumed electric parameters with a shield box which we made. We were able to presume electric parameters for diamagnetic materials with high accuracy. But our presumed electric parameters for ferromagnetic materials were less accurate. Since the nominal values of electric parameters are determined for the direct current case, it is not clear how significant is our comparison of the nominal values and our presumed values.

In the future, we want to theoretically presume the characteristics of a shielding material actually used in our society and to experimentally evaluate it.

7. Reference

[1] I.Nagano, Y.Yoshiura, S.Yagitani, T.Tosaka "Estimation of Electric Parameters of Thin Electromagnetic Shielding Materials" IEEJ Trans. FM. vol.123, no.2, pp.192-199, February 2003.